Infection of phytoplankton by aerosolized marine viruses

Shlomit Sharoni[a,b,1], Miri Trainic[a,1], Daniella Schatz[b], Yoav Lehahn[a], Michel J. Flores[a], Kay D. Bidle[c], Shifra Ben-Dor[d], Yinon Rudich[a], Ilan Koren[a,2], and Assaf Vardi[b,2]

Departments of [a]Earth and Planetary Sciences, [b]Plant and Environmental Sciences, and [d]Biological Services, Weizmann Institute of Science, Rehovot 76100, Israel; and [c]Institute of Marine and Coastal Sciences, Rutgers University, New Brunswick, NJ 08901

Edited by James L. Van Etten, University of Nebraska–Lincoln, Lincoln, NE, and approved April 10, 2015 (received for review December 10, 2014)

Marine viruses constitute a major ecological and evolutionary driving force in the marine ecosystems. However, their dispersal mechanisms remain underexplored. Here we follow the dynamics of *Emiliania huxleyi* viruses (*Eh*V) that infect the ubiquitous, bloom-forming phytoplankton *E. huxleyi* and show that *Eh*V are emitted to the atmosphere as primary marine aerosols. Using a laboratory-based setup, we showed that the dynamic of *Eh*V aerial emission is strongly coupled to the host–virus dynamic in the culture media. In addition, we recovered *Eh*V DNA from atmospheric samples collected over an *E. huxleyi* bloom in the North Atlantic, providing evidence for aerosolization of marine viruses in their natural environment. Decay rate analysis in the laboratory revealed that aerosolized viruses can remain infective under meteorological conditions prevailing during *E. huxleyi* blooms in the ocean, allowing potential dispersal and infectivity over hundreds of kilometers. Based on the combined laboratory and in situ findings, we propose that atmospheric transport of *Eh*V is an effective transmission mechanism for spreading viral infection over large areas in the ocean. This transmission mechanism may also have an important ecological impact on the large-scale host–virus "arms race" during bloom succession and consequently the turnover of carbon in the ocean.

algal bloom | aerosol | marine viruses | coccolithophores | *Emiliania huxleyi* virus

Oceanic phytoplankton blooms are the major primary producers that constitute the base of marine food webs, and are key components of large biogeochemical cycles in the ocean (1). *Emiliania huxleyi* (Prymnesiophyceae, Haptophyta) is a dominant, bloom-forming phytoplankton that plays a pivotal role in carbon and sulfur cycles owing to its high productivity, calcification rates, and DMS production and emission to the atmosphere (2–4). In recent years it has become evident that *E. huxleyi* blooms are largely influenced by the activity of *Eh*V, a lytic large double-stranded DNA coccolithovirus (Phycodnaviridae) that specifically infects *E. huxleyi* cells, accelerating the turnover and determining the fate of phytoplankton biomass (5–7). Bloom dynamics in the ocean is often characterized by a rapid demise of *E. huxleyi* cells owing to viral infection (5–10) that occurs over thousands of kilometers. Until recently, virus dispersal was thought to be solely mediated by physical processes within the water body, such as diffusion, advection, and mixing (11, 12). Recently, it has been shown that zooplankton can further enhance viral dispersal (13). These viral-dispersal mechanisms are restricted to processes within the water body. Recent evidence suggests that marine primary aerosols produced by wind-induced bubble bursting in the ocean (14) can be highly enriched with microorganisms (15–19). Nevertheless, there is very limited information on the presence of aerosolized marine viruses and their possible role as a transmission mechanism affecting large-scale host–virus interactions during algal bloom succession.

Results

***E. huxleyi* and *Eh*V Dynamics in Culture and Airborne *Eh*V Quantification.** Here we test the hypothesis that *Eh*V can be aerosolized by wind-induced bubble bursting and infect its *E. huxleyi* host after atmospheric transport and deposition. We established a laboratory-based setup in which we grew *E. huxleyi* in a continuously bubbled tank to mimic primary aerosol formation by bubble bursting (*SI Materials and Methods* and Fig. S1). The cultures were infected with *Eh*V, and viral emission to the air was quantified throughout the course of infection, along with sampling of host and virus abundances in the culture media. Following viral infection of the culture, the host's cell concentration declined (Fig. 1*A*), and was accompanied by an exponential increase in viral production that reached a maximal concentration of ~10^9 viruses per mL in the culture media (Fig. 1*B*). Concomitantly, *Eh*V concentration in the air increased and reached maximal concentrations of ~10^3 viruses per mL of air (Fig. 1*C*). Viral abundance in the air was shown to closely follow the virus concentration in the seawater with an average air-to-seawater ratio of 1:10^6. In the control experiment, where *E. huxleyi* was not infected, cells continued to grow exponentially and there was no viral production in the seawater and no emission of viruses into the air (Fig. 1 *A–C*, green line). To explore the morphology of the airborne *Eh*V particles, we examined the collected *Eh*V aerosols by transmission electron microscopy (TEM) imaging. The TEM micrographs clearly captured the typical icosahedral structure and dimensions (160–180 nm in diameter) of *Eh*V. Furthermore, some

Significance

Marine viruses constitute a major ecological and evolutionary driving force in marine ecosystems and are responsible for cycling of major nutrients; however, their dispersal mechanisms remain underexplored. By using one of the most established host–pathogen planktonic model systems we provide strong evidence that specific viruses of marine coccolithophores can be transmitted and stay infective as marine aerosols. Being transported by the wind, phytoplankton viruses can be conveyed long distances and transmit the infection to remote locations to which coccolithophore blooms can be extended. We show that this effective transmission mechanism that has been studied in human, animal, and plant diseases could play an important role in host–virus dynamics during phytoplankton blooms in the ocean.

Author contributions: I.K. and A.V. conceived the basic ideas and supervised the project; S.S., M.T., Y.L., Y.R., I.K., and A.V. developed the concept and designed experiments; S.S. and M.T. performed experiments; D.S., Y.L., M.J.F., and S.B.-D. performed additional lab, in situ and satellite analyses; K.D.B. was the chief scientist on the NA-VICE cruise; and S.S., M.T., I.K., and A.V. wrote the paper.

The authors declare no conflict of interest.

This article is a PNAS Direct Submission.

Freely available online through the PNAS open access option.

Data deposition: The sequences reported in this paper have been deposited in the GenBank database (accession nos. KJ820817–KJ820822).

[1]S.S. and M.T. contributed equally to this work.

[2]To whom correspondence may be addressed. Email: ilan.koren@weizmann.ac.il or assaf.vardi@weizmann.ac.il.

This article contains supporting information online at www.pnas.org/lookup/suppl/doi:10.1073/pnas.1423667112/-/DCSupplemental.

ENVIRONMENTAL SCIENCES

ECOLOGY

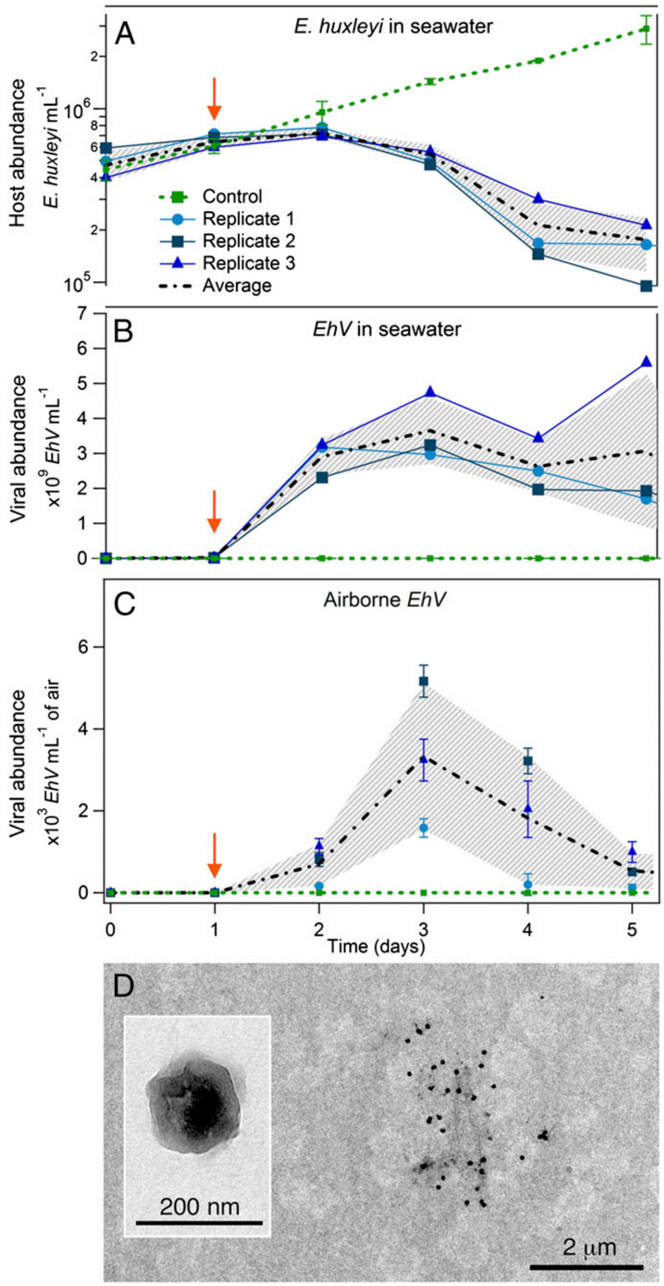

Fig. 1. Host–virus dynamics in infected *E. huxleyi* culture media and in emitted *Eh*V-containing aerosols. *E. huxleyi* host abundance (*A*) and *Eh*V abundance (*B*) in the culture media, and *Eh*V abundance in the collected aerosols (*C*). The orange arrows represent the time of viral addition to the culture media. The average of three replicates (blue lines) is presented by the dashed black line. The shadowed area represents the standard deviation of the three replicates' average. The green line is the control experiment using a noninfected *E. huxleyi* culture. (*D*) Aggregates of *Eh*V collected from aerosols emitted from the infected culture. No *Eh*V was observed in aerosols emitted from the noninfected culture.

of the airborne *Eh*V appeared in aggregates (Fig. 1*D*), which may alter their residence time in the atmosphere and susceptibility to abiotic conditions by providing physical protection.

Viral Infectivity of Aerosolized Viruses. To test whether the aerosolized viruses are infective, we linked the outflow of the bubbling system containing infected *E. huxleyi* culture using the previous setup to the headspace of two noninfected *E. huxleyi* cultures (Fig. 2*A*). These targeted cultures consisted of *E. huxleyi* strain RCC 1216, which is susceptible to *Eh*V infection, and a resistant strain, RCC 373. The latter served as a control host to validate that if cell lysis occurs it is triggered only by infective aerosolized *Eh*V, and not by other contaminants (20) (*SI Materials and Methods*). In the susceptible targeted host, *E. huxleyi* cells grew to densities of $\sim 1 \times 10^6$ cells per mL before cell lysis occurred 3 days after the initial exposure to the aerosols emitted from the infected culture source (Fig. 2 *B* and *C*). Concomitantly, virus concentration in the culture media of the target susceptible host increased to a maximal value of $\sim 6 \times 10^9$ viruses per mL. In contrast, the resistant target *E. huxleyi* cells continued to grow rapidly, reaching a concentration of $\sim 4 \times 10^6$ cells per mL, and no viral production was detected (Fig. 2 *B* and *C*). These findings indicate that aerosolized *Eh*V remain infective when transmitted through air and can lead to efficient lysis of noninfected adjacent *E. huxleyi* populations. Furthermore, we tested the infectivity of aerosolized viruses at lower aerial concentrations that are more ecologically relevant (~10–100 viruses per L of air) and found similar results (*SI Materials and Methods*, Figs. S2 and S3, and Table S1).

Decay Rate of Airborne *Eh*V. Unlike the laboratory system, viruses in the natural atmosphere may become inactive owing to structural damage upon exposure to UV radiation and changes in temperature and relative humidity (21, 22). To estimate the time scale over which *Eh*V can remain infective in the atmosphere, we measured viral decay rate after exposure to atmospheric conditions typical for daytime clear-sky North Atlantic spring blooms. We used the most probable number (MPN) method (23) for calculations of viral infectivity and found that *Eh*V infectivity decays exponentially with a calculated decay rate of k = $\sim 0.033\ \text{min}^{-1}$, corresponding to a half-life time of 20 min (Fig. 3). This decay rate was detected under simulated atmospheric conditions of temperature15.9 ± 0.2 °C, relative humidity 65–75%, and light intensity 700 μmol photons$\cdot$m$^{-2}\cdot$s^{-1} provided by a halogen lamp with a spectrum simulating sunlight (400–700 nm) (*SI Materials and Methods*). This result is comparable to previous studies that reported nonmarine viruses can remain infective in the atmosphere for several hours (23–26). In addition, the half-life of infectious *Eh*V in the ocean under similar prevailing condition is, as expected, much longer, ~35 h (13). Unlike bacteria and algae, viruses have no active DNA repair systems; consequently, their inactivation rates are usually higher than those of other microorganisms (25). Nevertheless, they may remain infective for a longer time during nighttime or overcast conditions, when they are not exposed to radiation. Therefore, we hypothesize that our calculated half-life for clear-sky daytime conditions represents a lower limit of the time that *Eh*V can remain infective in the marine atmosphere.

Detection of Airborne *Eh*V over a Natural Bloom in the North Atlantic. To assess the ecological significance of our laboratory findings under natural algal bloom conditions, we examined aerosol samples collected during an *E. huxleyi* spring bloom in the North Atlantic (*SI Materials and Methods*). The aerosols were collected on July 3 and 4, 2012, at a sampling site where high abundance of *E. huxleyi* cells ($\sim 1.4 \times 10^3$ cells per mL, Fig. 4*C*) and *Eh*V ($\sim 5 \times 10^4$ *Eh*V per mL, Fig. 4*C*) were observed in the top 40 m of the water column (location: 61.90°N, 33.70°W). These values were associated with similar patterns of chlorophyll fluorescence (Chl) and particulate inorganic carbon (PIC) retrieved from the moderate resolution imaging spectroradiometer (MODIS) aqua satellite (Fig. 4 *A* and *B*). The satellite images, together with high *E. huxleyi* and *Eh*V abundances in the water column, were indicative of an active viral infection during *E. huxleyi* bloom (10). TEM analysis of collected aerosol samples revealed large virus-like particles (LVLPs) with morphology and size comparable to

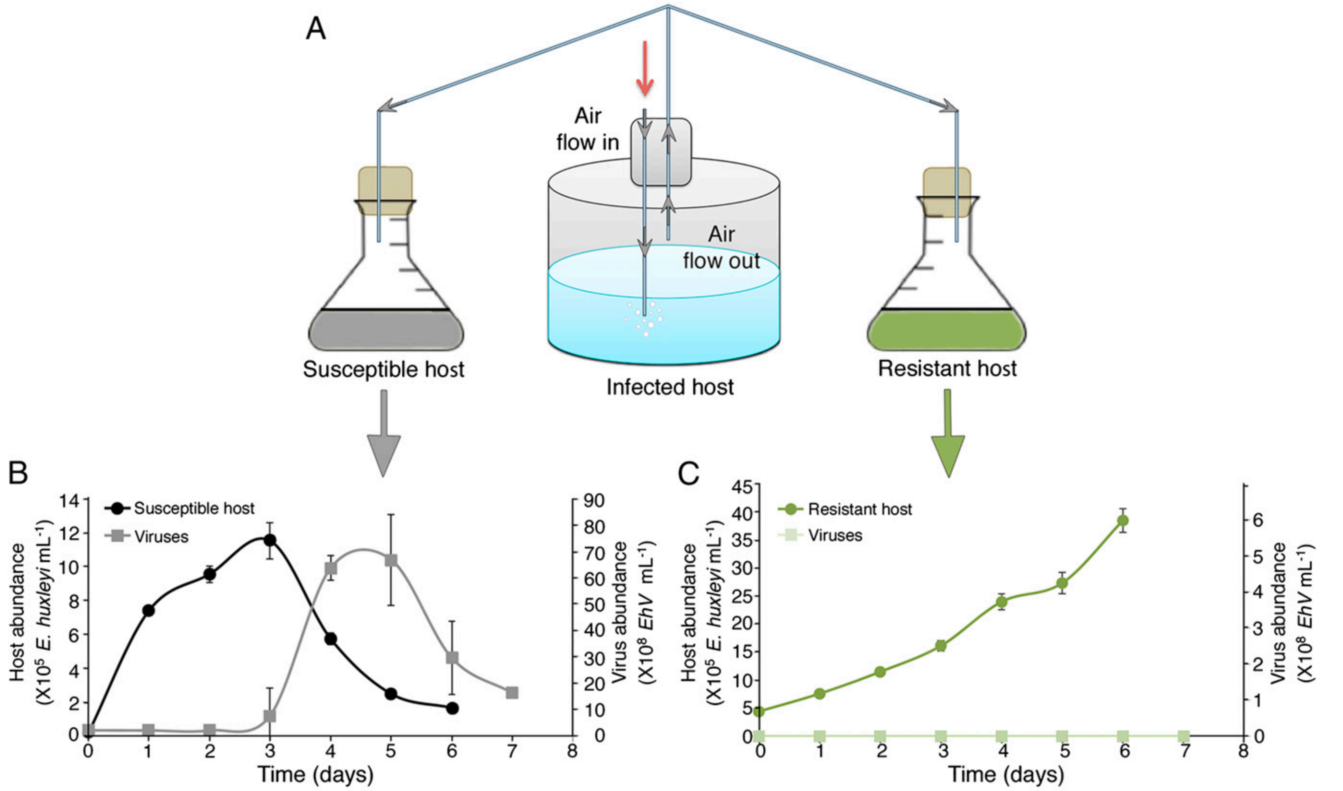

Fig. 2. Aerosolized *Eh*V infecting healthy *E. huxleyi* populations. (*A*) Experimental setup: Aerosolized viruses from an infected culture were continuously directed into the headspace of new, healthy *E. huxleyi* cultures. Host–virus dynamic was followed in (*B*) a susceptible *E. huxleyi* culture ($n = 4$), and in (*C*) a resistant *E. huxleyi* culture ($n = 2$). Error bars represent the SD of the biological replicates.

those of *Eh*V (Fig. 4*D*). Furthermore, a clear *Eh*V DNA signature was obtained from these collected aerosol samples, when using specific primers to the conserved viral phosphoglycerate mutase (PGM) gene in PCR analysis. These primers were used extensively to examine viral diversity in the ocean (27). Phylogenetic analysis of the PGM sequences clearly identified these amplicons as *Eh*Vs that cluster together with other known *Eh*V-PGM sequences but are significantly different from them (Fig. 4*E* and Fig. S4). An *Eh*V with an identical PGM sequence was isolated from seawater samples at 50 m depth on the same cruise (13).

Meteorological data revealed that on the same dates and location about half of the time the wind speed exceeded the minimum threshold of 4 $m \cdot s^{-1}$ for marine aerosol production by bubble bursting (28). Therefore, it is reasonable to assume that the *Eh*V found in the aerosol samples is likely to be emitted from nearby *Eh*V-rich seawater (28).

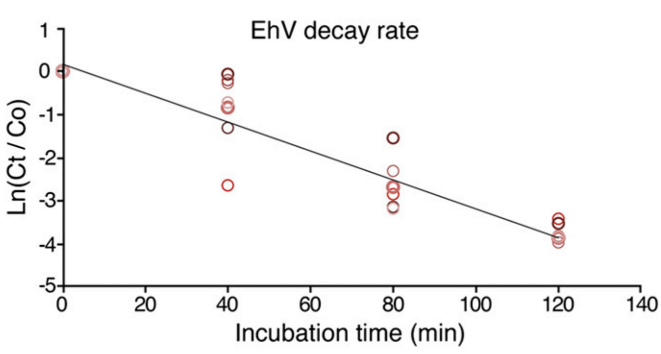

Fig. 3. Decay rate of *Eh*V. *Eh*Vs were exposed to atmospheric conditions that prevail during *E. huxleyi* blooms in the North Atlantic (temperature 15.9 ± 0.2 °C, relative humidity 65–75%, light intensity 700 μmol photons$\cdot m^{-2} \cdot s^{-1}$). The *y* axis is the natural logarithm (ln) of the fraction of remaining infective viruses (presented as C_t/C_0), where C_0 is the MPN of infective viruses at time 0 and C_t is the most probable number of infective viruses at time *t* ($n = 7$). The black line represents the linear fit of the replicates' average. $Y = -0.0335x + 0.1676$, $R^2 = 0.9818$.

Discussion

Although virus-like particles were previously found in marine aerosols (15, 18), our study presents conclusive genetic and morphological evidence for primary emission of viruses infecting a specific bloom-forming algal host. Furthermore, we suggest that such emissions to the atmosphere may play a critical role in the dispersal of viral infection over large-scale *E. huxleyi* blooms in the ocean (10).

To estimate the potential extent of infection dispersal following *Eh*V emission, we performed a calculation combining our laboratory and in situ findings. We found that for an average wind velocity (∼8 $m \cdot s^{-1}$, *SI Materials and Methods* and Table S2) *Eh*V concentration in the air is expected to be six orders of magnitude less than its abundance in the water (Fig. 1 *B* and *C* and Fig. S5). Our in situ measurements revealed that during an open ocean *E. huxleyi* bloom, *Eh*V can reach seawater concentrations of $\sim 10^4$ *Eh*V per mL (Fig. 4*C*). Therefore, under close to steady-state conditions, we can estimate the *Eh*V concentration in the lower atmospheric boundary layer to be ∼10 viruses per L of air. Although a typical *E. huxleyi* bloom occupies thousands of square kilometers (29), we consider only a limited area of 1 km^2 of sea surface and 10 m of a well-mixed atmosphere above it, yielding a parcel of 10^{10} L of air with an estimated *Eh*V population of over 10^{11} aerosolized *Eh*V. Using 20 min as the lower limit for the

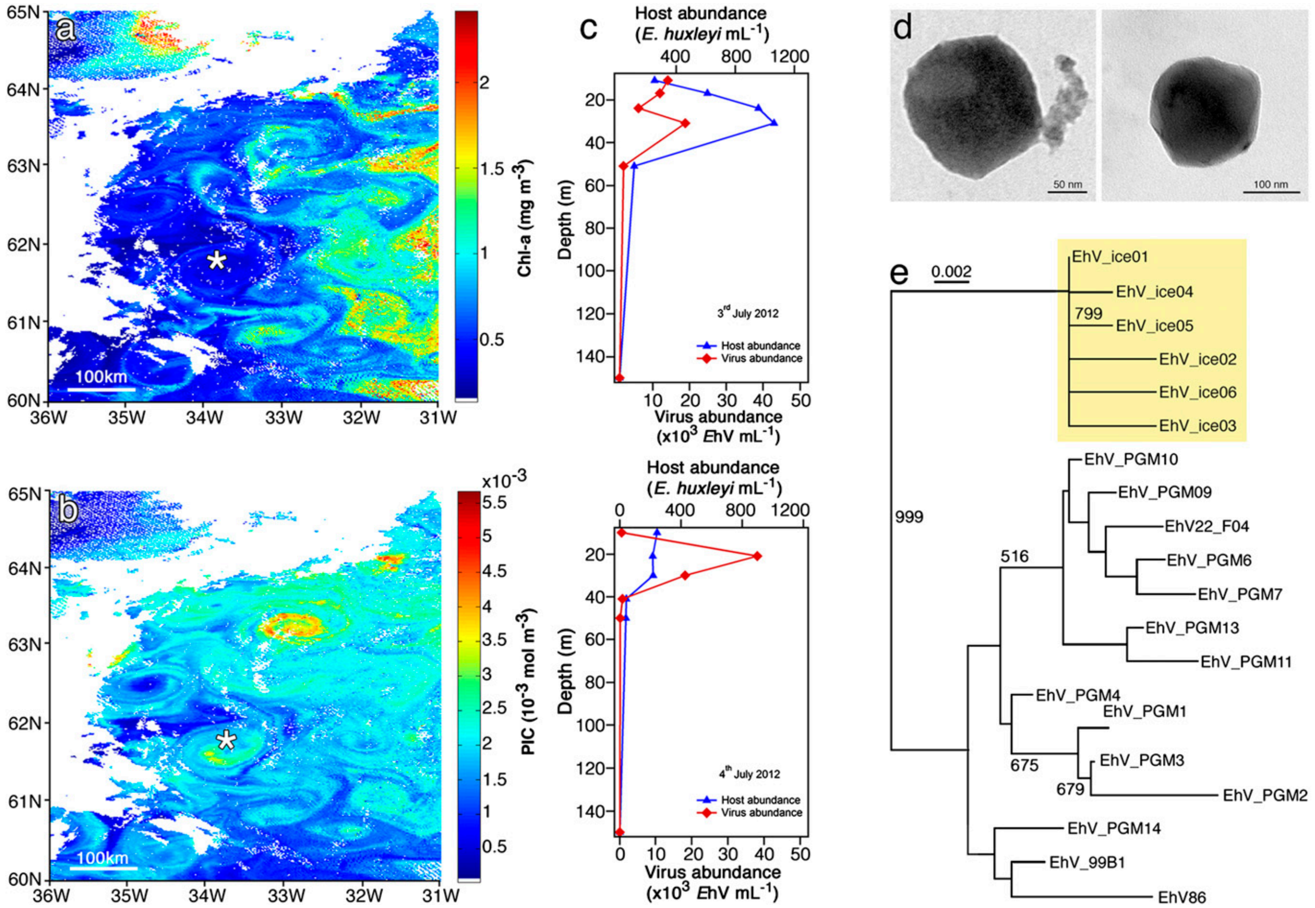

Fig. 4. *Eh*V detection in seawater and in aerosols during an *E. huxleyi* North Atlantic spring bloom. MODIS aqua satellite imagery of (*A*) Chl-a and (*B*) PIC at the sampling location (white star, 61.90°N, 33.70°W, on July 3 and 4, 2012). (*C*) Seawater profiles of *E. huxleyi* and *Eh*V concentrations from July 3 (*Top*) and 4 (*Bottom*), 2012. (*D*) TEM images of LVLPs found in the aerosol samples. (*E*) Neighbor-joining tree based on *Eh*V genotypes (PGM gene) from the aerosols. Distinct *Eh*V groups obtained from the aerosol samples are labeled as PGM *Eh*V_ice 01–06 (highlighted in yellow); bootstrap values above 500 are presented.

*Eh*V half-life (under daytime atmospheric conditions, Fig. 3), we calculate that the infective virus concentration will be reduced by an order of magnitude within 1 h. Moreover, owing to the high dilution factor in the atmosphere, and the long lifetime of submicron aerosols, only a small fraction of the airborne *Eh*V is expected to be deposited back to the ocean within 1 d (30, 31). Mayol et al. (32) have recently reported that ∼10% of microbes in the atmospheric boundary layer were airborne for 4 d post-emission, traveling up to 11,000 km before deposition. Using 7 $m \cdot s^{-1}$ as the typical surface wind speed over the North Atlantic (28) we estimate that an air parcel with 10^{11} viruses can disperse through the air and convey 10^7 infective viruses after traveling for hundreds of kilometers. A case study over the measurement area for July 3, 2012, revealed a very consistent wind trajectory for 12 h, suggesting that that the emitted virus particles are likely to be advected over narrow sectors for several hours and therefore most of the deposition would be concentrated over it (Fig. S6 and *SI Materials and Methods*).

Dispersal through wind-driven processes may contribute to fast and efficient infection at higher rates than other dispersal mechanisms such as diffusion, mixing, advection, and currents (33). Although estimation of dispersal of passive tracers in the ocean is challenging, most estimations suggest that the characteristic distances by which the released viruses will spread per unit of time will be orders of magnitude smaller in the water than through the air. For example, tracing the propagation of an iron-fertilized patch in the Southern Ocean (34) showed a dispersal scale of 150 km after 6 weeks, which is comparable to 1-d dispersal in the atmosphere. In cases where algal blooms are confined to patches in the open ocean (10), the best measure for dispersion accounting for turbulence is defined as eddy diffusivity (35). Considering viral release from infected cells as a passive tracer, the characteristic propagation velocity of the front of the volume containing the tracers can be estimated as the ratio between the characteristic eddy diffusivity coefficient to the characteristic length scale. It was shown that the high-end values of the eddy diffusivity coefficient are on the order of 1,000 $m^2 \cdot s^{-1}$ for scales of 10–100 km, yielding a propagation velocity in the order of ∼1 $cm \cdot s^{-1}$ for a 100-km scale, as opposed to ∼1–10 $m \cdot s^{-1}$ in the atmosphere (35, 36).

The difference between the two transport processes is of two to three orders of magnitude, indicating that aerial dispersal can be an efficient transmission mechanism, which can contribute to the observed large-scale, rapid, and synchronized *E. huxleyi* bloom demise attributed to viral infection (5, 6, 9, 10).

Therefore, we suggest that aerosolization and consequent aerial dispersal can be a common mechanism for epidemics of marine pathogens. These findings may have important implications for the factors determining microbial composition, flow of nutrients in marine food webs, and large biogeochemical cycles in the ocean (37, 38).

Materials and Methods

The experimental setup and the methods are described fully in *SI Materials and Methods*.

E. huxleyi and _Eh_V Dynamics in the Culture and Airborne _Eh_V Quantification. Four liters of *E. huxleyi* susceptible strain RCC 1216 cultures were grown in a 10-L carboy in f/2 media and infected with *Eh*V201 during the exponential growth phase. Simultaneously, a control culture that was not infected was grown under the same conditions. Cultures were continuously bubbled at a rate of 3 $L \cdot min^{-1}$. The emitted aerosols from the infected and the control cultures were collected on nitrocellulose filters every 24 h, extracted, and analyzed for viral DNA abundance. Quantification of *Eh*V in the culture and in the aerosols was determined by quantitative PCR (qPCR) for the *Eh*V major capsid protein gene (MCP). *E. huxleyi* cell analysis was performed with an Eclipse (iCyt) flow cytometer.

Viral Infectivity of Aerosolized Viruses. Similar to the previous experiment, 4 L of *E. huxleyi* susceptible strain RCC 1216 cultures were grown and continuously bubbled in a 10-L carboy in f/2 media and infected with *Eh*V201 during the exponential growth phase. The outflow from the carboys containing the infected cultures was split with a stainless steel flow splitter into two 2-L Erlenmeyer flasks, each containing 1 L of *E. huxleyi* culture. One Erlenmeyer flask contained the susceptible *E. huxleyi* RCC 1216 strain ($n = 4$), and the other contained the resistant *E. huxleyi* RCC 373 strain ($n = 2$). The cultures were further incubated for 5–6 d postexposure to airflow from the infected carboy. The resistant strain was used to demonstrate that the demise is due to viral infection and not due to other stresses or toxic contaminants rising from the infected population in the carboy. Cultures were harvested for cell and viral enumeration in the carboy and in the two Erlenmeyer flasks every 24 h. Host and virus quantification was performed as described above.

Decay Rate Experiment. *Eh*V201 was introduced onto polyester filters using a vacuum pump. The filters were incubated under regulated atmospheric conditions as follows: temperature 15.9 ± 0.2 °C, 65–75% relative humidity, light intensity of 700 $\mu mol \cdot m^{-2} \cdot s^{-1}$ (400–700 nm). Filters were collected at different time points: 0, 40, 80, and 120 min ($n = 7$). Viruses were extracted from the filters, and a series of 10-fold dilutions were used to infect host cultures ($n = 12$). After incubation we used the MPN method (23) to determine the number of infective viruses at each point.

Oceanographic Cruise Water and Air Sampling. Water was collected from 61.90°N, 33.70°W on July 3 and 4, 2012, during the North Atlantic Virus Infection of Coccolithophore Expedition (NA-VICE; KN207-03, www.bco-dmo.org/project/2136), aboard the R/V *Knorr*. Water samples were obtained from the water column using a Sea-Bird SBE 911plus CTD carrying 10-L Niskin bottles, and genomic DNA was isolated from filtered biomass using an adapted phenol–chloroform method. Air was continuously collected during the cruise by pulling through PM10 inlet heads placed on a 15-m-high ship mast. Aerosols were collected for 24 h on 47-mm nitrocellulose and PVDF filters and kept at 4 °C until analysis. DNA from the collected filters was extracted and tested for the presence of *Eh*V using primers designed for the PGM gene (Fig. 3).

ACKNOWLEDGMENTS. We thank the captain and crew of the R/V *Knorr*; the Marine Facilities and Operations at the Woods Hole Oceanographic Institution for assistance and cooperation at sea; and Miguel Frada, Orr Shapiro, and Uria Alcolombri, as well as all members of A.V. group, for comments on the manuscript. We are grateful to Haya Avital from the Design, Photography and Printing Branch at the Weizmann Institute of Science for assistance with preparation of the figures. All TEM studies were conducted at the Moskowitz Center for Bio-Nano Imaging at the Weizmann Institute of Science. This research was supported by European Research Council (ERC) StG (INFOTROPHIC) Grant 280991 (to A.V.), National Science Foundation (NSF) Grant OCE-1061883 (to A.V.), and the ERC under the European Union's Seventh Framework Programme (FP7/2007-2013)/ERC Grant 306965 (CAPRI) (to I.K.) The research cruise was supported by NSF Grant OCE-1061883 (to K.D.B. and A.V.).

1. Behrenfeld MJ, et al. (2006) Climate-driven trends in contemporary ocean productivity. *Nature* 444(7120):752–755.
2. Balch WM, Holligan PM, Ackleson SG, Voss KJ (1991) Biological and optical properties of mesoscale coccolithophore blooms in the Gulf of Maine. *Limnol Oceanogr* 36(4):629–643.
3. Beaufort L, et al. (2011) Sensitivity of coccolithophores to carbonate chemistry and ocean acidification. *Nature* 476(7358):80–83.
4. Simó R (2001) Production of atmospheric sulfur by oceanic plankton: Biogeochemical, ecological and evolutionary links. *Trends Ecol Evol* 16(6):287–294.
5. Jacquet S, et al. (2002) Flow cytometric analysis of an *Emiliana huxleyi* bloom terminated by viral infection. *Aquat Microb Ecol* 27(2):111–124.
6. Wilson WH, Tarran G, Zubkov MV (2002) Virus dynamics in a coccolithophore-dominated bloom in the North Sea. *Deep Sea Res Part II Top Stud Oceanogr* 49(15):2951–2963.
7. Vardi A, et al. (2012) Host-virus dynamics and subcellular controls of cell fate in a natural coccolithophore population. *Proc Natl Acad Sci USA* 109(47):19327–19332.
8. Bratbak G, Egge JK, Heldal M (1993) Viral mortality of the marine alga *Emiliania huxleyi* (Haptophyceae) and termination of algal blooms. *Mar Ecol Prog Ser* 93(1–2):39–48.
9. Ziveri P, Broerse ATC, van Hinte JE, Westbroek P, Honjo S (2000) The fate of coccoliths at 48°N 21°W, Northeastern Atlantic. *Deep Sea Res Part II Top Stud Oceanogr* 47(9–11):1853–1875.
10. Lehahn Y, et al. (2014) Decoupling physical from biological processes to assess the impact of viruses on a mesoscale algal bloom. *Curr Biol* 24(17):2041–2046.
11. Murray AG, Jackson GA (1992) Viral dynamics: A model of the effects of size, shape, motion and abundance of single-celled planktonic organisms and other particles. *Mar Ecol Prog Ser* 89(2):103–116.
12. McManus MA, Woodson CB (2012) Plankton distribution and ocean dispersal. *J Exp Biol* 215(Pt 6):1008–1016.
13. Frada MJ, et al. (2014) Zooplankton may serve as transmission vectors for viruses infecting algal blooms in the ocean. *Curr Biol* 24(21):2592–2597.
14. Lewis ER, Schwartz ES (2004) Fundamentals. *Sea Salt Aerosols Production: Mechanisms, Methods, Measurements and Models*, eds Lewis ER, Schwartz ES (American Geophysical Union, Washington, DC), Vol 152, pp 17–39.
15. Aller JY, Kuznetsova MR, Jahns CJ, Kemp PF (2005) The sea surface microlayer as a source of viral and bacterial enrichment in marine aerosols. *J Aerosol Sci* 36(5):801–812.
16. Baylor ER, Baylor MB, Blanchard DC, Syzdek LD, Appel C (1977) Virus transfer from surf to wind. *Science* 198(4317):575–580.
17. DeLeon-Rodriguez N, et al. (2013) Microbiome of the upper troposphere: Species composition and prevalence, effects of tropical storms, and atmospheric implications. *Proc Natl Acad Sci USA* 110(7):2575–2580.
18. Leck C, Bigg EK (2005) Biogenic particles in the surface microlayer and overlaying atmosphere in the central Arctic Ocean during summer. *Tellus* 57(4):305–316.
19. Prather KA, et al. (2013) Bringing the ocean into the laboratory to probe the chemical complexity of sea spray aerosol. *Proc Natl Acad Sci USA* 110(19):7550–7555.
20. Paytan A, et al. (2009) Toxicity of atmospheric aerosols on marine phytoplankton. *Proc Natl Acad Sci USA* 106(12):4601–4605.
21. Jensen MM (1964) Inactivation of airborne viruses by ultraviolet irradiation. *Appl Microbiol* 12(5):418–420.
22. Tang JW (2009) The effect of environmental parameters on the survival of airborne infectious agents. *J R Soc Interface* 6(6, Suppl 6):S737–S746.
23. Taylor J (1962) The estimation of numbers of bacteria by tenfold dilution series. *J Appl Microbiol* 25(1):54–61.
24. Donaldson AI (1972) The influence of relative humidity on the aerosol stability of different strains of foot-and-mouth disease virus suspended in saliva. *J Gen Virol* 15(1):25–33.
25. Després VR, et al. (2012) Primary biological aerosol particles in the atmosphere: A review. *Tellus* 64:15598.
26. McDevitt JJ, Milton DK, Rudnick SN, First MW (2008) Inactivation of poxviruses by upper-room UVC light in a simulated hospital room environment. *PLoS ONE* 3(9):e3186.
27. Coolen MJ (2011) 7000 years of *Emiliania huxleyi* viruses in the Black Sea. *Science* 333(6041):451–452.
28. Lehahn Y, et al. (2014) Decoupling atmospheric and oceanic factors affecting aerosol loading over a cluster of mesoscale North Atlantic eddies. *Geophys Res Lett* 41(11):4075–4081.
29. Tyrell T, Merico A (2004) *Emiliania huxleyi*: Bloom observations and the conditions that induce them. *Coccolithophores: From Molecular Processes to Global Impact*, eds Thierstein HR, Young JR (Springer, Berlin), pp 75–99.
30. Saltzman SE (2009) Marine aerosols. *Surface Ocean—Lower Atmosphere Processes*, eds Le Quéré C, Saltzman SE (American Geophysical Union, Washington, DC), Vol 187, pp 17–39.
31. Vignati E, et al. (2010) Global scale emission and distribution of sea-spray aerosol: Sea-salt and organic enrichment. *Atmos Environ* 44(5):670–677.
32. Mayol E, Jiménez MA, Herndl GJ, Duarte CM, Arrieta JM (2014) Resolving the abundance and air-sea fluxes of airborne microorganisms in the North Atlantic Ocean. *Front Microbiol* 5:557.
33. McCallum H, Harvell D, Dobson A (2003) Rates of spread of marine pathogens. *Ecol Lett* 6(12):1062–1067.
34. Abraham ER, et al. (2000) Importance of stirring in the development of an iron-fertilized phytoplankton bloom. *Nature* 407(6805):727–730.
35. Marshall J, Shuckburgh E, Jones H, Hill C (2006) Estimates and implications of surface eddy diffusivity in the Southern Ocean derived from tracer transport. *J Phys Oceanogr* 36(9):1806–1821.
36. Ledwell JR, Watson AJ, Law CS (1998) Mixing of a tracer in the pycnocline. *J Phys Oceanogr* 103(C10):21499–21529.
37. Danovaro R, et al. (2011) Marine viruses and global climate change. *FEMS Microbiol Rev* 35(6):993–1034.
38. Suttle CA (2007) Marine viruses—major players in the global ecosystem. *Nat Rev Microbiol* 5(10):801–812.

ENVIRONMENTAL SCIENCES

ECOLOGY